Ballistic magnetoresistance?

2008 J. Phys.: Condens. Matter 20 083201

(http://iopscience.iop.org/0953-8984/20/8/083201)

J. Phys.: Condens. Matter **20** (2008) 083201 (18pp) doi:10.1088/0953-8984/20/8/083201

TOPICAL REVIEW

Ballistic magnetoresistance?

B Doudin[1] **and M Viret**[2]

[1] Institut de Physique et de Chimie des Matériaux de Strasbourg (IPCMS), UMR 7504 CNRS-ULP, 67034 Strasbourg, France
[2] Service de Physique de l'Etat Condensé, DSM/DRECAM-CNRS URA 2464, CEA Saclay, 91191 Gif-sur-Yvette cedex, France

Received 26 September 2007, in final form 24 October 2007
Published 1 February 2008
Online at stacks.iop.org/JPhysCM/20/083201

Abstract
We review the published work on electric transport in metallic magnetic nanocontacts of sizes reaching a single atom. Considering fabrication methods exempt from mechanical instabilities, we find two experimental consensuses in magnetoresistance measurements. Firstly, magnetoresistance does not exceed a few tens of per cent in atomic size constrictions. We attribute these modest values to the significant number of opened conduction channels expected in contacts of 3D metals. Secondly, anisotropic magnetoresistance is observed for all types of samples, with amplitudes at least one order of magnitude larger than those found in bulk samples. Abrupt resistance changes with field angle confirm the occurrence of discrete anisotropic magnetoresistance levels. The effect is attributed to enhanced spin–orbit coupling at the atomic scale, resulting in possible opening or closure of conductance channels when varying the angle between current and applied magnetic field.

(Some figures in this article are in colour only in the electronic version)

Contents

1. Introduction

Electric transport in heterogeneous magnetic materials is nowadays an established research topic in magnetism. The use of the spin of the conduction electrons opens new possibilities for electronic devices, including sensors, memories, and logic applications, motivating worldwide research activity. For metallic systems, progress in thin film fabrication makes possible the realization of magnetic heterogeneous structures, where the magnetization orientation can be controlled over short length scales, down to the nanometre range. If a modification of the magnetization configuration can be realized within a distance over which the conduction electrons keep the memory of their spin orientation (reaching several hundreds of nanometres), a related change of resistance of the sample occurs. For the majority of the systems involving transition metals, a diffusive conduction model applies, owing to the sample size being larger than the electronic mean free path (usually not exceeding 10 nm). The related so-called giant magnetoresistance (GMR) properties are well understood within a phenomenological model involving parallel current channels carried by the two spin populations with spin-dependent scattering in the bulk and at interfaces [1–3].

The phenomenology and understanding of GMR drastically change for samples of ultimate dimensions smaller than the electron mean free path. In this ballistic regime of conduction, one expects the band structure of the material to govern the magnetoresistance (MR) properties. Schep *et al* pioneered the idea, showing how GMR can rely on band structure, without introducing spin-dependent diffusion [4, 5]. They motivated experiments, aiming at performing mechanical point contact [6] transport on magnetic multilayers. The disappointing findings [7, 8] were essentially attributed to mechanical disruptions of the layered structure, limiting the interest of this technique for understanding GMR. The topic was revived with spectacular MR properties found by Garcia's group on simple Ni contacts, using mechanical methods to approach two wires of micron to millimetre-range diameters [9]. Further extensions showed similar behaviour on electrodeposited Ni contacts [10–12], and other reports using similar mechanical techniques confirmed the results on a variety of ferromagnetic systems [13, 14]. The observation of MR ratios reaching a few hundred per cent, larger than reported GMR amplitudes, was interpreted in terms of resistance values strongly modified when the mutual magnetic alignment of the two wires in contact changes from parallel to antiparallel and was used as a justification of the denomination of 'ballistic magnetoresistance' (BMR). A significant interest in the community was also motivated by fundamental questions: can a magnetic domain wall width, usually significantly larger than the electronic mean free path ℓ in such metals, become restrained by the length of a constriction, supposedly smaller than ℓ [15, 16]? Can a process of ballistic transport through a domain wall result in enhanced MR ratios [17–22]? Reports of huge MR effects in electrodeposited nanocontacts triggered enormous publicity, fuelled by the perspective of a new generation of spin electronics devices [23–25]. However, several research groups encountered difficulties when trying to reproduce such experiments. The dispute reached a climax in conferences in 2004 [26], in particular in a dedicated 'Symposium on the Controversy Over Ballistic Magnetoresistance' at the Ninth Intermag Conference (Anaheim, CA, January 5–9, 2004). A consensus emerged for criticizing reported results on BMR, invoking essentially the lack of control of mechanical artefacts potentially biasing the results, reaching the conclusion that: 'It is entirely possible that there is no real BMR effect of any significant magnitude in any previously published data' [27].

In the last decade, significant improvements in nanofabrication methods provided adequate tools for fabricating controllable electrical connections of nanometre dimensions. For metallic conductors of size reduced down to a few atoms, the ballistic properties are expected to govern electric transport properties. When constrictions reach the de Broglie wavelength of conduction electrons, the wave nature of the electrons restricts their transmission by allowing only certain modes to propagate, resulting in a discrete nature of the conductance. Even though the required dimensions for metals reach atomic limits, there is a consensus in the literature that such behaviour can be observed up to room temperature.

The purpose of this review is to discuss a number of experimental set-ups and findings, motivated by initial experiments on BMR, and designed for optimum mechanical stability and/or control. The first section will briefly summarize the basic formalism and key theoretical ingredients for understanding ballistic transport. We will focus on the application to magnetic materials, as more exhaustive information regarding normal metals and superconductors can be found elsewhere [28]. The next section will review the different nanofabrication strategies found in the literature, each having its own advantages and disadvantages, providing several different approaches to the same problem. Section 3 will present the experimental findings, from which an initially unexpected picture emerges. Large BMR values cannot be reproduced in experiments minimizing mechanical artefacts, which is a disappointing conclusion confirming the doubts on initial BMR experiments. However, a large anisotropy in the MR of the contacts is systematically observed, of magnitude and angular properties very distinct from bulk materials. Section 4 will be dedicated to reviewing experimental findings and theoretical concepts used to understand anisotropic magnetoresistance, and the difference between diffusive and ballistic regimes. Close interaction between experimentalists and theorists results in clearer experimental design and results. Such findings provide a unique insight into the modification of MR properties when approaching the atomic-size limit. This understanding is a key for future electronic devices, for which the atomic-size control is recognized as the ultimate bottleneck for device miniaturization [29]. This review will also underline that understanding of experimental results is still subject to controversy, as mechanical contributions to MR properties cannot be fully excluded when studying samples made of a few atoms and subject to a significant applied magnetic field. This is therefore not a closed topic, but the research status is now advanced enough to ensure unambiguous identification of the important sample parameters, as well as identifying clearly what are the stability and reproducibility limits of atomic-size samples for spin electronics applications.

We will limit our discussion to metallic devices. The most convincing experiments of ballistic transport are however performed on semiconductors, as the sample size restrictions are less stringent than those required for metals. Ballistic injection of spins [30] and spin–orbit coupling [31] are essential ingredients for making efficient semiconductor devices taking advantage of the spin of current carriers. The concepts developed in this review are therefore of importance for other types of systems, for which dedicated reviews can be found in the literature [32, 33].

2. Theoretical summary

2.1. Ballistic transport formalism

Ohm's law states that when an electric field is applied onto a conductor the current density that passes through it is linear with the applied voltage and is inversely proportional to the conductor's length and proportional to its cross section. These properties are known to hold well for macroscopic samples, for which the conductor's size is much greater than some relevant length scales. For very small samples, Ohm's law

breaks down and other electrical transport regimes take place. The longest length scale is the coherence length, L_ϕ, which is the average distance a conduction electron travels between two inelastic scattering events. Between two such consecutive events, only elastic collisions occur and the electron keeps its phase. Hence, any theoretical description of transport below this scale involves taking into account the wave nature of the particles. In particular, experiments designed to underline the relevance of the phase (like the Aharonov–Bohm effect) have demonstrated that interferences between different conducting paths can indeed be important at this length scale. The next smaller length scale corresponds to the average distance in between two scattering events, ℓ. Below this, in a classical vision of transport, the trajectory of the electrons remains unperturbed by any scattering. This is the ballistic regime of conduction. In the macroscopic diffusive regime, because the current flowing through the sample depends on the number of scattering events, the sample's resistance is proportional to the conductor's length, whereas in the ballistic regime the resistance falls to zero. The total sample resistance results from the boundaries between the ballistic channel and the leads, where thermal equilibrium is attained through scattering events. These boundaries are the regions where electronic wavefunctions are back-scattered before flowing freely in the channel. At low temperature in metals the order of magnitude for the mean free path and the coherence length are respectively several tens of nanometres and a few microns. In the ballistic regime, the important parameter of a model system composed of leads connecting a conducting channel is the diameter, $2a$, of the entrance to the channel. The resulting conductance G was calculated by Sharvin, who pointed out the analogy with the problem of a dilute gas passing though a small hole [34]. The current density is the product of the charge of the electron with the average group velocity in the direction normal to the aperture ($hk_F/2m$), and the density of states ρ_F at the Fermi level (mk_F/π^2h^2). Realizing that the volume density of particles contributing to electronic transport corresponds to $\rho_F eV/2$, one can integrate the current density over a disc of radius a, and deduce a conductance

$$G = 2e^2/h(\pi a/\lambda_F)^2. \tag{1}$$

In this semi-classical treatment, within the adiabatic approximation, one rather strong hypothesis is taken, that of non-correlated collisions during electronic transport. This is no longer correct when coherent interferences from back-scattering become non-negligible and one has to take into account quantum effects, such as weak localization and universal conductance fluctuations. Another hypothesis, that electrons can be treated as corpuscular entities, requires a radius a much larger than the electron's wavelength λ_F. This implies that the conductance of such a system is much larger than $2e^2/h$ ($\approx 1/12\,900\ \Omega^{-1}$), which is the benchmark value of quantum effects.

The ultimate length scale corresponds to the wavelength of the conduction electrons (λ_F) and requires a wave-type treatment of electron transport between the two sides of such a microscopic sample. This resembles wave propagation in guides where the channel width is of the order of the wavelength of the incident wave. In metals, where the number of charge carriers is comparable to the number of constituent atoms, the conduction electrons' Fermi wavelength is of the order of the interatomic distance, i.e. a few Å.

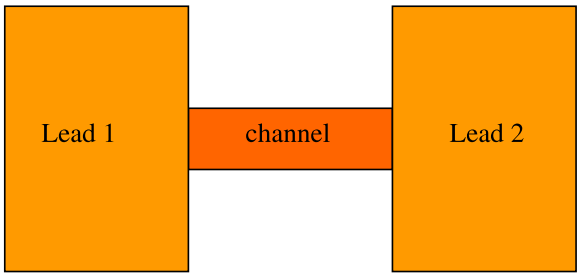

Figure 1. The principle schematic diagram of a two-terminal one-dimensional (1D) ballistic conductor.

In order to calculate the conductance of these small systems, Landauer introduced the idea that in the absence of any inelastic scattering the conductance can be expressed in terms of a scattering matrix S of the sample [35]. The simplest example of mesoscopic conductor is modelled by two perfect leads connecting a narrow channel as in figure 1. The electrodes act as ideal electron reservoirs in thermal equilibrium with a well defined temperature, resulting in chemical potentials μ_1 and μ_2. Due to lateral confinement in the leads, the transverse momentum of electrons is quantized (as in an infinite potential well of width w), which defines independent longitudinal channels along which electrons propagate as plane waves. The conductance calculation reduces to the evaluation of ordinary transmission T and reflection R coefficients of the sample as in elementary quantum mechanics. In the simplest case of a perfect one-dimensional conductor, the product of the velocity and one-dimensional density of states simplifies to $2/h$. There, the conductance is found to be

$$G_0 = 2e^2/h, \tag{2}$$

called the quantum of conductance. The fact that a perfect single-mode conductor between two leads has a finite resistance given by a universal quantity is in disagreement with the classical intuition, where one expects to have zero resistance for the perfectly conducting case. This illustrates the idea of a finite resistance arising from the thermalization of ballistic electrons in the reservoirs through scattering events. For a larger sized perfect one-dimensional channel, the conductance is found to be given by the number of propagating modes each carrying a conductance quantum. Hence, in this simple model, conductance is quantized in multiples of G_0.

Model experiments were carried out on two-dimensional semiconductor electron gases (2-DEG) [36, 37], taking advantage of the rather large charge carriers Fermi wavelength, and the possibility to tune electrostatically the width of the contact. A similar quantization was then found for metallic systems [38] at low temperatures. A large literature can be found on metallic systems (mainly Au), where repetitive contact-breaking experiments are used to extract a statistical

indication that simple multiples of G_0 are more likely to occur (see a review in [28]). Conductance measurements performed when visualizing Au contacts in an electron microscope at room temperature [39] provide direct evidence that indeed quantized conductance appears when the size of the junction is of a few atoms, with a tendency to form atomic 'wires', i.e. lines of a few atoms connecting the two electrodes.

More generally, if one considers transport through a non-ideal 1D channel, where scattering events are therefore allowed, each conduction channel i transmits only a fraction $T_i < 1$ of the incoming current, while the reflected part is soaked up by the reservoirs. In this more general multi-channel case, the conductance can be expressed as

$$G = \frac{2e^2}{h} \sum_{i=1}^{N} T_i \tag{3}$$

with a summation performed on all propagating channels i. The existence of conduction channels relates to the presence of wavefunctions at the Fermi energy. For the simplest 1D case, the number of conduction channels results from the number of intersecting branches of a 1D dispersion curve with the Fermi energy. For metallic systems, the occurrence of single-channel conduction is thus expected in monovalent metals. Moreover, realistic geometries for atomic-size contacts can deviate significantly from a periodic 1D system, resulting in non-perfect transmission factors. It has indeed been shown theoretically and experimentally that perfect single-channel conduction is rather rare and limited to monovalent and s-type electron metals like Au [40, 41]. The full atomic orbital overlap and bonding has to be considered in describing realistic atomic-sized contacts. When doing so, it appears that the number of conducting channels is roughly of the order of the number of valence electrons. Transmission factors can also depend sensitively on the exact geometry of the contact and the orbitals considered. Hence, it should be underlined that conductance quantization in an integer number of G_0 is only obtained for idealized 1D systems. In fact, it can be shown that transmission factors vary continuously with orbital overlap: if it were possible to continuously change the interatomic distance between two central atoms of an atomic chain, the conductance would smoothly decrease. Thus, it is likely that conductance steps are associated with the stability of some specific atomic configurations rather than a signature of quantized transport.

2.2. Application to magnetic materials

The quantum of conductance includes a factor of two, related to the spin degeneracy of the conduction electrons. It is possible to lift this degeneracy, for example by applying a large magnetic field with a resulting Zeeman splitting of energy larger than $k_B T$. Magnetic materials have the particularity of their band structure being split by a large exchange energy. Conducting channels are therefore spin dependent and the (true) conductance quantum is e^2/h. Hence, in the case of single-channel conduction, electronic transport would be fully polarized and the material would become (locally) a half-metallic conductor [42]. Such a property represents the 'Holy Grail' of spin electronics, allowing amplification of MR values and ideal spin injection [32]. In the ideal case of a single, hence fully polarized, conduction channel between two ferromagnetic electrodes, the direction of magnetizations on both sides will sensitively affect the transmission. When the magnetizations are parallel the conductance is e^2/h, but in the antiparallel case electrons can be fully reflected because this spin-up channel is non-propagating in the down-magnetized region. Hence, magnetoresistance would be expected to reach extremely large values when the sample resistance is of the order of 10^4 Ω [19, 43].

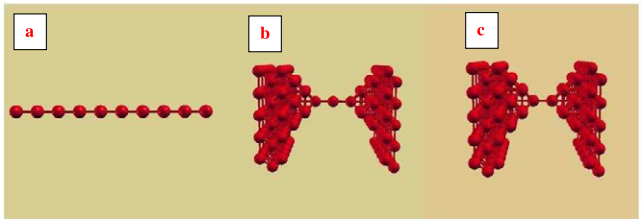

Figure 2. Illustration of different atomic configurations considered for theoretical calculations.

As already mentioned and illustrated in the next experimental sections, it is unclear if magnetic nanocontacts of high transmission factors can be made [28]. This would require making a 1D wire, without imperfections, with a diameter smoothly increasing when connected to the diffusive banks. As far as 3D atomic contacts are considered, the atomic configurations obtained in break junction experiments are likely to consist of complicated shapes touching on one or a few atoms. Figure 2 illustrates how one can model a contact geometry different from the perfect transmission case, and provide a good pedagogical example of the importance of the atomic configuration. For the infinite 1D wire (figure 2(a)), the calculation of the density of states and consequently the magnetic moment on the atoms is feasible in a fully *ab initio* manner. It is found that for Fe the spin moment is 3.2 μ_B per atom, significantly higher than the 2.25 μ_B of the bulk, as expected in an object of reduced dimensionality [44]. From the density of states, one can infer in a very direct manner the conductance. Indeed, for such a perfect, completely periodic, system, each band crossing the Fermi level contributes e^2/h to the conductance. For the infinite Fe wire, one finds that seven bands cross the Fermi level, hence the conductance should be $7e^2/h$. This is a much higher value than the conductance quantum and, as regards spin polarization, six of these channels have spin down and one has spin up. Thus, the carrier spin polarization is 85%. Generally speaking, the s bands are expected to exhibit limited spin splitting, which always prevents a full spin polarization. When one gets away from the ideal 1D geometry, things change quite dramatically. For example, the two configurations of figures 2(b) and (c) lead to conductance values between e^2/h and $2e^2/h$. At first sight, it is surprising that structures with cross sections everywhere larger than the atomic wire can be about five times less conducting. This is actually a good illustration of the breakdown of Ohm's law in this regime of transport. As stated before, there is a geometrical mismatch between the leads

and the atomic contact that reflects electron wavefunctions. Moreover, in the case of non-periodic systems, electrons are scattered everywhere in the contact and transmittances differ from zero or one. Generally speaking, in these atomic structures, one cannot expect conductance to be quantized in simple e^2/h multiples.

Large MR ratios potentially obtained when going from parallel to antiparallel alignments of the two sides of the contacts are only expected when the local magnetization changes abruptly by 180° between two neighbouring atoms. This situation is not expected, as the exchange energy in the atomic chain opposes the anisotropy to define the length on which magnetization rotates, and involves typically at least 10^2 atoms in bulk materials. Initial spectacular experiments motivated more detailed calculations of the possible occurrence of atomic-size domain walls in ferromagnets [15, 16, 45–47]. These are usually found to be a few atoms long, which results in small total transmission changes. Therefore, MR due to magnetization non-collinearity in atomic contacts is not expected to be large, and typical reasonable values should be around 10–20%, expected when closing or opening one or two conduction channels among at least five total open channels [45, 47].

3. Fabrication techniques

This section describes three different methods used for making atomic-sized contacts, with documented results on ferromagnetic systems under applied external magnetic field. A significant motivation for performing the experiments was to limit the influence of mechanical effects. Magnetostatic forces, magnetoelastic modifications of the electrodes and the resulting strains on the substrate can affect the configuration and environment of a nanocontact when the magnetization orientations of the two sides of the contact change. This review will not enter into the details of such calculations, which can be found elsewhere [27, 48, 49]. It is intuitively clear that any change of magnetic configuration should be reflected by a relative change of length $\Delta l/l$, where l is the freestanding length of the samples. If a sample is anchored at its two extremities, the thin nanocontact (or nanogap) region absorbs all the absolute Δl value, resulting in MR properties potentially revealing breaking and opening of a contact by mechanical constraints. A trivial way to reduce Δl is to diminish l, by 'sticking' the contacts as best as possible to a substrate, keeping the shortest possible freestanding fraction of the device. All the described experiments in this section limit l to below 100 nm, and the resulting Δl to values below 0.01 nm.

3.1. Mechanical break junctions (MBJs)

This fabrication technique, originally invented by van Ruitenbeek *et al* [50], relies on a precise breaking of a metallic film by bending a flexible substrate on which the material has previously been deposited. This is clearly the most documented method for fabricating atomic contacts [28].

A metallic nanostructured bridge is defined by e-beam lithography onto a flexible substrate (for instance kapton) onto

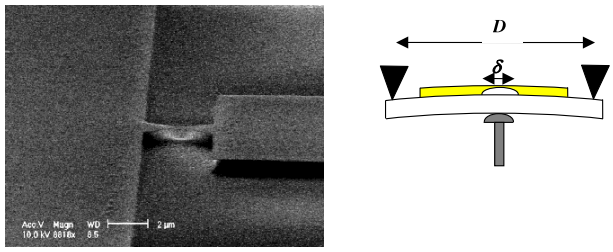

Figure 3. Left: scanning electron microscope picture of a mechanical break junction. The undercut below the bridge localizes the breaking area. Right: schematic diagrams of the junction design, involving a pushing bottom vertical rod with the black arrows corresponding to the anchoring points separated by a distance D in the centimetre range. The undercut has a length δ in the micrometre range.

which a micron-thick layer of polyimide has been previously spun. The bridge is suspended by reactively etching the polyimide (figure 3). By bending the substrate, a strain is applied on the bridge, which can then break, and be brought back to contact. The resistance is monitored during the breaking process, which can be stopped and reversed at any time, thereby allowing a large number of measurements to take place and providing a convenient statistical tool. The extreme stability of the set-up is due to the fact that the metal is everywhere attached to the substrate (except under the bridge), thus not allowing independent motion of the electrodes. Its sensitivity results from the very large ratio between the breaking mechanism (three studs separated by typically 1 cm) and the under-etching below the bridge (typically 1 μm). Hence, the ratio between bending and the distance that electrodes are pulled apart allows control of the pulling distance in the 10 pm range [50]. The junction can be installed in a cryostat with ultra-high vacuum capabilities where both low temperature and high purity can be realized when making and breaking the contacts. With this set-up, it is possible to stabilize an atomic contact for hours, or even days. This is desirable for MR measurements because one needs to sweep a significant external magnetic field while measuring resistance, a procedure that can take several minutes. The MBJ technique has unique advantages in terms of stability, suitability for low-temperature studies and versatility for repetitive closing and opening of an atomic contact. There is however, a limited literature on performing it on transition magnetic metals. One possible reason might be the lack of statistical occurrence of quantized steps of the conductance when performing extensive statistics [51]. It has recently been shown that H_2 or CO molecules can significantly change the statistics, revealing that UHV conditions are of importance, and that surface impurities can drastically alter the experimental data [52].

Another set-up allowing mechanical breaking of nanocontacts consists of an STM tip which can be controllably extended and retracted onto a metallic thin film. This system has the advantage of not requiring patterning of the sample, but does not allow long-term stability. It provides therefore access to statistics on breaking a junction, without (until now) the capability to study the samples under variable applied magnetic

fields, as mechanical artefacts might bias the results. Results on magnetic systems can be found in the literature, where reports of quantized conductance can be found [53, 54]. When mounted inside an electron microscope, the set-up allows one to image the neck of the breaking. Beautiful atomically resolved images can clearly demonstrate the atomic character of the contacts before breaking. In Au, chains have been shown to form and the conductance monitored in real time follows very well the different stages of breaking [39, 55]. This technique has also been applied to magnetic materials, and the observation of quantized conductance of e^2/h steps has been reported (somewhat in contradiction with the theoretical considerations of the previous section!) [56]. The imaging capability of the system is a clear advantage over most other set-ups, but has not been shown to be compatible with MR investigations.

3.2. Electrical break junctions (EBJs)

This method relies on electromigration triggered by large current densities on a patterned neck of a thin metallic line (figure 4). This strategy, pioneered by Park *et al* [57], is becoming increasingly popular for fabricating ultra-thin gaps for the purpose of single-molecule transport studies [58–60]. It is readily compatible with a bottom gate configuration, allowing three-terminal measurements to be performed, of key importance for electrical spectroscopic studies. E-beam lithography is typically used to pattern the adequate thin metallic line with a constriction providing a limited area where the current density is highest. The irreversibility of the process limits its statistical use, but a large number of samples can be patterned on a given chip, allowing many single attempts. This fabrication can also be performed in UHV and cryogenic conditions. One should mention that the adequacy of such electrodes for convincing transport measurements is still a source of debate, owing to the questionable structural quality of the electrodes (due to the thin films needed to trigger a breakage) [61, 62], and the possible occurrence of metallic clusters during the electromigration [63–65], possibly due to excessive heating during the breaking process [66, 67]. Such problems limit the number of successful samples, complicating and confusing the result interpretation. The intense research activity is evolving towards better understanding and control of the process [68, 69], but often revealing that initial results might have been over-optimistic. There are a few reports on the use of such a method in the quantum ballistic regime of conduction [70–72], owing to the difficulty in stabilizing closed electrical contacts. One definitive advantage of this method is that no freestanding length of the sample should be present, which is of high interest for MR studies.

3.3. Electrochemical junctions (ECJs)

Combining physical and chemical techniques is an attractive method to make nanocontacts. This family of samples is intrinsically very different from those obtained by mechanical or electric break methods. The environment is an electrochemical bath, normally involving an aqueous ionic solution. The experiments are performed around ambient

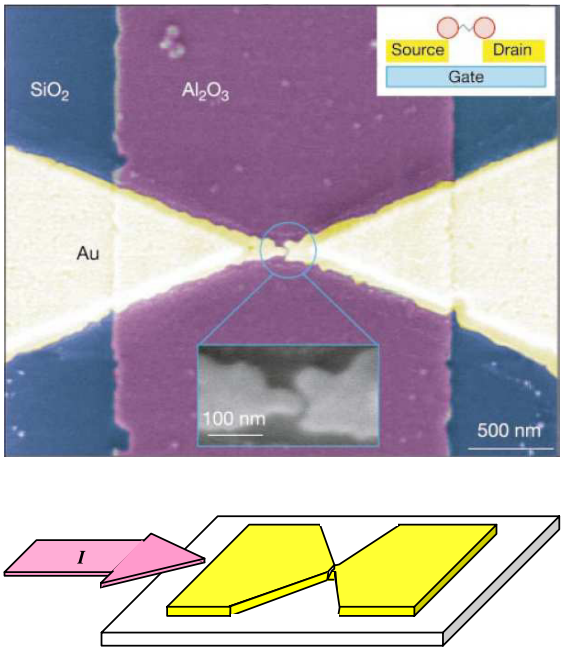

Figure 4. Scanning electron microscope picture of an electrical break junction. Reprinted by permission from Macmillan Publishers Ltd: Nature [58]. ©2002.

temperature, far from the cryogenic conditions of the other samples.

This technique was originally reported by Morpurgo *et al* for making Au contacts [73], using e-beam lithography to pattern two nearby electrodes, typically separated by a distance of 100 nm. Electroplating was used to fill the gap, keeping a monitoring of the inter-electrode resistance during sample growth and revealing quantized steps of the conductance for Au nanocontacts when closing the gap (figure 5). Refinements in the deposition [74] and techniques [75], involving high-frequency impedance monitoring [76, 77] or bipotentiostatic control [78], can be found in the literature. Repetitive closing and opening of a gap can be realized by adequate tuning of the electrode potential, under the condition that no other chemical reactions occur on the electrode surface. This opens the possibility of statistical studies. However, this method is often more fastidious than MBJ, and limited statistics are shown in the literature [79, 80]. The electrolytic conditions also complicate the interpretation of the statistics [81]. One interest of the ECJ is that the electrodes where the metal is deposited or stripped (the so-called working electrodes) can have a controlled potential value, fixing the Gibbs potential of the chemical reaction. This ensures for example that no oxygen is stabilized at the electrode surface during the sample growth, and also enforces the direction of the chemical reaction, with expected high purity of the junctions. This method does not provide long-term stability of few-quantum conductance occurrence, normally limited below 100 s. The electrolyte of significant conductivity, necessary for the electrochemistry to take place, limits the use of this type of junctions for tunnel measurements between electrodes, but should not contribute significantly when the conductance reaches e^2/h. The ECJ also has unique advantages, in particular by allowing

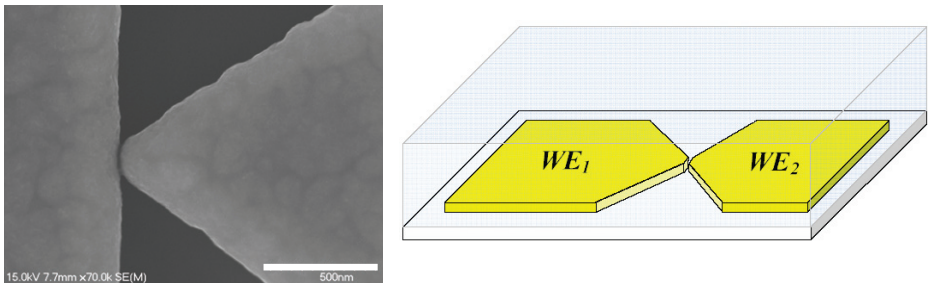

Figure 5. Scanning electron microscope picture of an electrochemical junction, with 500 nm scale bar (from [49]). Right: scheme of the junction, with the two working electrodes (WE1 and WE2), immersed in an electrolyte, as indicated by the shaded volume.

fabrication of heterogeneous systems, made of two different materials as contact electrodes [82]. This technique is also ideally suited for room-temperature studies, which is difficult for EBJs because of the low-temperature fabrication and substrate dilatation when heating up to room temperature. ECJs are also attractive for MR studies, owing to their limited freestanding section, and the 'constructive' method used to make the junctions. This is in contrast to the breaking techniques, mostly investigating a system at its weakest point.

This electrochemical fabrication method is often categorized as 'easy', which is a claim revealing its non-(electro)chemist origin! Cathodic reduction of transition metal ions on a metallic substrate is a complicated process, usually involving adsorption of hydrated ionic species, and often a multi-step reduction or oxidation process [83]. The limited experimental details and information on the electrochemical conditions of the substrate are often limiting the reproducibility of the experiments and the progress in the field. A popular method for fabricating nanocontacts, aiming at improving the time stability of the samples, relies on the so-called 'self-termination' technique [84]. It uses one of the electrodes forming the contact as a counter-electrode, and a shunt resistor in series to stabilize the nanocontact resistance by adjusting the potentials of the two sides of the contact. In our opinion, this technique is not adequate for transition metal deposition/dissolution, as it enforces an oxidation reaction on one side of the contact to compensate for the reduction occurring on the other side. In layman terms, this set-up maximizes the chemical contamination of the contact, which is evidently highly undesirable.

Finally, one should realize that the ECJ does not result in pure contacts. It is for example unavoidable to produce hydrogen during the deposition of ferromagnetic contacts, as the hydrogen reduction potential $2H^+ + 2e^- \rightarrow H_2$ is less negative than reduction of Fe, Co or Ni ions (except in the case of so-called under-potential deposition, occurring for a few monolayers on the adequate substrate, therefore not relevant to the presented experiments). For example, it has been shown that increasing the hydrogen evolution during Ni plating results in conductance statistics of the ECJ nanocontacts consistent with those measured in MBJs under H_2 atmosphere, and showing clearer occurrence of quantum conductance multiples [52]. One should therefore keep in mind that ECJs are expected to exhibit properties significantly different from the other types of junctions.

3.4. Concluding comments

Several other attempts for making magnetic nanocontacts can be found in the literature, with a stability criterion reasonably fulfilled. The nanopore fabrication method [85], or direct e-beam fabrication of constrictions [86], provide stable systems, but limited data on conductance properties near the quantum limit can be found on the literature.

We want to emphasize that all presented techniques have their advantages and disadvantages. To summarize, one can fairly state that the MBJ is the best-understood fabrication technique and provides optimum purity, but is potentially sensitive to mechanical artefacts. Without the under-etching stage, it has been shown however that magnetostriction has a negligible effect on the MBJ, of the same order as the other presented methods. Because one pulls on the atoms to break the junction, this presumably leads to the stabilization of non-thermodynamically stable configurations, for instance with unusual bond lengths (especially at low temperatures). It is indeed harder to observe clear discrete conductance behaviour when making atomic contacts this way. The EBJ method is in its infancy, has good mechanical, purity and low-temperature controls, but is irreversible and might also suffer from intrinsic unstable connection, for example due to disorder, which limits the reproducibility of the experiments. The ECJs are significantly different samples, owing to their room-temperature and liquid environment. This can be seen as a disadvantage in terms of studying a well defined sample in the cleanest environment, or as an advantage in the perspective of creating applicable devices and stabilizing the surface. ECJs have good mechanical and electrical stability making them of interest for MR studies, but are of limited purity.

Our purpose is not to indicate which fabrication method is good or not, or what is the best fabrication strategy. Our aim is to emphasize that these samples are intrinsically quite different. We therefore hope to obtain complementary information resulting from the experimental results, or get more confidence in the results if common conclusions are drawn from significantly different samples and environments.

4. Magnetoresistance properties

Experiments investigating the change of resistance under sweeping applied magnetic field have been performed for the three types of samples previously described.

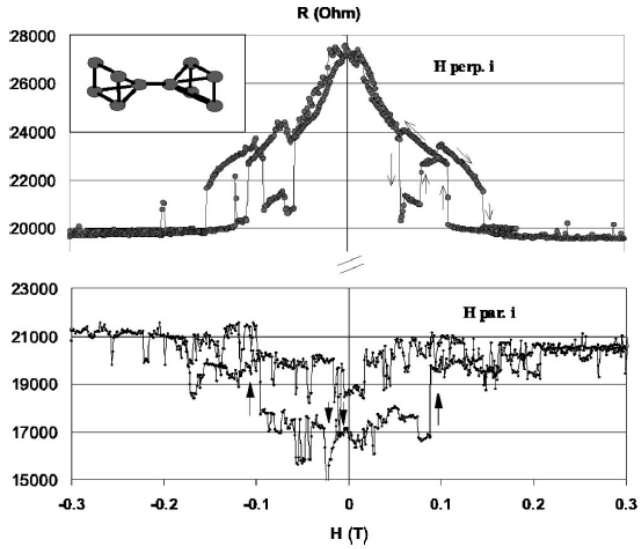

Figure 6. Magnetoresistance properties of a Ni junction obtained by a mechanical breaking technique, measured at 17 K. Reprinted figure with permission from [87]. Copyright 2002 from the American Physical Society.

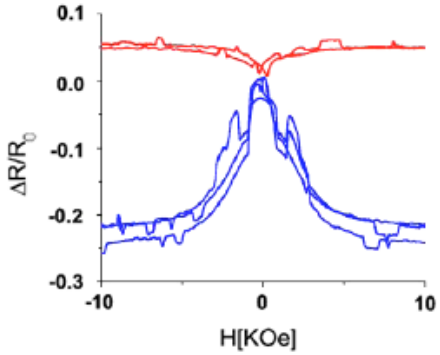

Figure 8. Magnetoresistance properties of a Ni junction obtained by electromigration, measured at 10 K, with two orientations of the applied magnetic field (top, in plane; bottom, out of plane). Reprinted with permission from [71]. Copyright 2007, American Institute of Physics.

The first report of MR studies in the quantum regime of conductance was presented by Viret *et al*, on Ni MBJs (figure 6) at low temperature (17 K). The set-up allowed stabilization of a contact in the tunnelling regime ($G < 0.1e^2/h$) and in the quantum regime ($G > 1.3e^2/h$), within a time frame allowing an external field to be swept [87]. They showed an MR effect of a few ten per cent, maximum when the samples had a conductance lower than a few quanta. Clear resistive indication of saturation of the effect was found, and the change of resistance could be explained by a change of relative magnetization of the two sides of the contact. The limited MR in the tunnelling regime was a clear argument against mechanical deformation of the sample. However, these initial experiments revealed rather noisy MR curves, and a limited number of successful samples.

Results on the ECJ were reported by Yang *et al* (figure 7) [79, 88], and Mallet *et al* [89], who also found limited MR values for Ni at room temperature. The experiment was performed *in situ* during fabrication and dissolution of the nanocontact, with adequate applied magnetic field sweep during stable plateau conductance values. The data allowed recording and direct comparison within a significant range of conductance values, by showing ΔG change when sweeping the field of the order of e^2/h, for G values between 1 and 100 e^2/h [88]. The MR ratio was maximal when the conductance was of the order of e^2/h, but found not to exceed 70%. The discussion of potential mechanical artefacts indicated that the shear of the metallic substrate was the potential main source of mechanical instabilities on these samples. A simple test, performed by varying the metallic composition of the initial electrodes (Au or Ni) indicated robust MR results [90]. The possibility to open and close the contact several times resulted in data corresponding to a significant number of reproducible experiments, allowing more confidence in the presented results.

Experiments preformed on EBJ samples at low temperatures by two independent groups confirmed the data of figures 6 and 7 (figure 8) [70, 71]. Again, the shapes of the MR curves

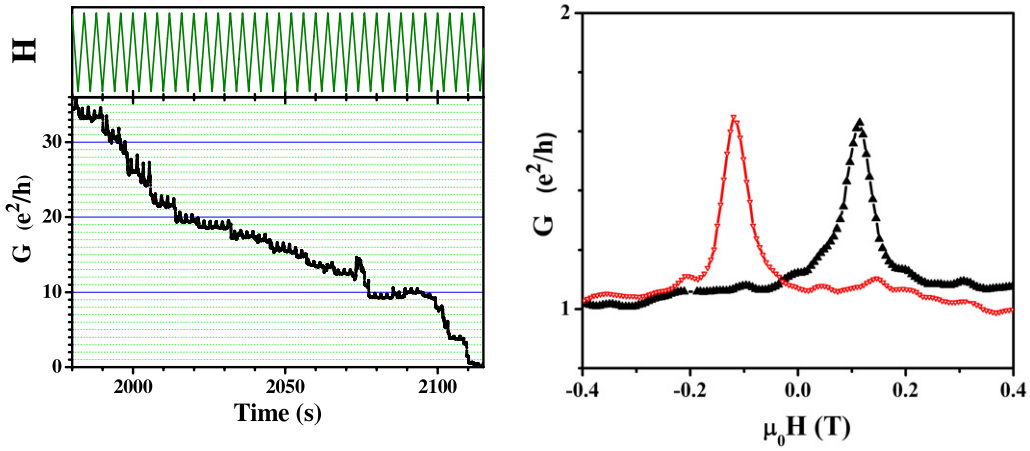

Figure 7. Magnetoresistance properties of a Ni junction obtained by electrodeposition, measured at 300 K. Left: the conduction versus time, under sweeping magnetic field (top zigzag line). Right: corresponding MR curve, of largest amplitude observed. Reprinted with permission from [88]. Copyright 2004, American Institute of Physics.

are similar to those found on MBJ and ECJ samples, with no MR values exceeding 80% observed.

Even though the fabrication, environment and measurement temperatures are different, all these results have remarkable significant common experimental findings;

- The magnitude of the MR does not correspond to reported results of amplitude much larger than giant MR ratios, i.e. larger than 100%. Such results confirm the claim of Egelhoff *et al* that data attributed to very large 'ballistic magnetoresistance' is unlikely to be correct [27].
- The shape of the MR curves is in first approximation similar for all temperatures and types of samples. This is a somewhat surprising result, as the shapes, aspect ratios and environments of the samples are different, and it is unexpected to find similarities in the magnetic properties. Yang *et al* observed similar MR curves when modifying significantly the shapes of the touching electrodes [88].
- The magnitude of the MR decreases rapidly with decreasing sample resistance. The conductance change under sweeping applied magnetic field is of the order of e^2/h, even though the conductance varies by up to two orders of magnitude. When reaching resistance values corresponding to typical Sharvin's resistance in a metal (several ohms), the expected MR values do not exceed the per cent range, in agreement with experiments using point contact geometry [85, 86, 91].

One can therefore fairly state that there is a strong experimental indication that no spectacular MR has been found in the ballistic regime of conduction, as revealed by extensive data on Ni and permalloy. In our opinion, the lack of very large MR properties is caused by the unlikely occurrence of samples involving a single channel of perfect transmission, and an atomic-sized domain wall width. The initial results showed either positive or negative MR curves [9–12, 23, 24], often without clearly explaining what might be the origin of the difference.

The observation of MR behaviour independent of the shape of the electrodes suggests that the MR properties were essentially controlled by the angle between magnetization and flowing current in the sample [88]. Such behaviour is analogous to the anisotropic magnetoresistance properties, where the sample resistance depends on the saturation magnetization direction. Figures 6 and 8 illustrate this hypothesis. The reported change of resistance under varying applied field could then be interpreted as resulting from a rotation of the magnetic moments in the contact region, without invoking the occurrence of a domain wall (or occurrence of local antiparallel magnetic configuration). This triggered interest in a new set of experiments, involving angular studies of the conductance on samples in a saturated magnetic state, or anisotropic magnetoresistance properties.

5. Anisotropic magnetoresistance

5.1. Anisotropic magnetoresistance in the diffusive regime (AMR)

Thomson showed in 1859 that the resistance of a ferromagnetic material depends on the mutual orientation of the applied magnetic field $\vec{H}$ and current $\vec{j}$ (figure 9) [92]. This so-called anisotropic magnetoresistance (AMR) relates therefore to the experimental indication that $\rho_{\parallel}$ ($\vec{H} \parallel \vec{j}$) is, in most cases, larger than $\rho_{\perp}(\vec{H} \perp \vec{j})$. It was only a century later that the effect was more thoroughly studied theoretically [93, 94] and experimentally [95–97]. Experimentally, it has been shown that starting from a truly randomly demagnetized state the resistivity generally increases for $\vec{H} \parallel \vec{j}$ and decreases for $\vec{H} \perp \vec{j}$, as schematically indicated in figure 9.

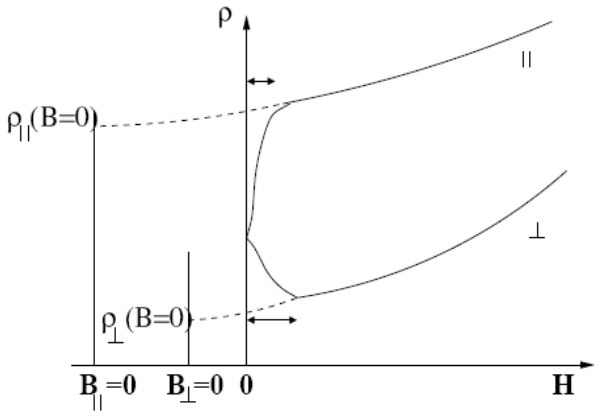

Figure 9. Schematic diagrams of the magnetic field induced resistive variations in ferromagnets. The anisotropy can be estimated by extrapolation of the curves to zero induction. Reproduced with permission from [97]. ©1976 Institute of Physics.

Galvanomagnetic effects are a property of magnetic materials. They are usually called 'extraordinary' or 'anomalous', in contrast to the so-called 'ordinary' MR. The latter (related to the dotted curves in figure 9) comes from the comparison with the behaviour of non-magnetic materials, showing a typical quadratic increase of the resistivity under large applied magnetic field. This is related to the Lorentz force $\vec{F} = q\vec{v} \times \vec{B}$ resulting on the charge carriers, which deflects charges from the current direction and causes a change in the longitudinal resistance of the material. The field can even trap the charge carriers in (closed) cyclotron orbits, removing their contribution to the current density until they are scattered. Hence, the resulting effect is significant only if the mean free path is comparable to the conduction electron's radius of curvature. As a result, the electrical resistance of non-magnetic metals increases in an applied magnetic field. The effect is also anisotropic because of the symmetry of the Lorentz force, resulting in transverse MR ($\vec{j} \perp \vec{M}$) slightly larger than the longitudinal one ($\vec{j} \parallel \vec{M}$). Note that free electron theory predicts zero MR and only by taking into account Fermi surface effects can one explain the normal Lorentz MR. The anomalous behaviour in ferromagnetic systems refers to the magnetic induction replaced by an internal field (the 'Weiss field') proportional to the magnetization of the sample. Thus, the ordinary galvanomagnetic effects come from the macroscopic part of the flux density $\mu_0 H_{\text{eff}}$, while the extraordinary effects stem from its microscopic part $\mu_0 M$. MR in ferromagnets can be phenomenologically expressed by the electric field $\vec{E}$ generated by a current density $\vec{j}$ in a magnetic

single-domain polycrystal:

$$\vec{E} = \rho_\perp(\vec{B})\vec{j} + [\rho_\parallel(\vec{B}) - \rho_\perp(\vec{B})](\vec{m}\cdot\vec{j})\vec{m} + \rho_H(\vec{B})\vec{B}\times\vec{j} + \rho_{\mathrm{AHE}}(\vec{B})\vec{m}\times\vec{j} \quad (4)$$

where $\vec{B}$ is the induction in the sample and $\vec{m}$ the unit vector in the direction of the magnetization. The first term is the Lorentz contribution to the MR, which depends on the cyclotron frequency and the mean free path. The second term depends on the orientation of the magnetization relative to the current direction. One defines the AMR as an intrinsic material property by considering the resistivities for $\vec{j}$ parallel and perpendicular to $\vec{m}$ at $B = 0$, as they do not depend on the details of shape and magnetization process of the sample. They experimentally follow the relation

$$\rho(\theta) - \rho_\perp = (\rho_\parallel - \rho_\perp)\cos^2\theta \quad (5)$$

where θ is the angle between the current and the magnetization. The third and fourth terms are the Hall effects which give the transverse contribution of the electric field. These are split into two parts; one is from the normal (Lorentz) effect and the other one is purely magnetic and called the 'anomalous Hall effect' or 'extraordinary Hall effect'. Here, we will neglect the influence of these transverse voltages when performing two-point measurements.

The mechanism by which the microscopic internal field associated with $\vec{M}$ couples to the current density in ferromagnets is the spin–orbit interaction between the electron trajectory (orbit) and the magnetization (spin). Thus, there is a fundamental difference between the classical nature of the ordinary effects and the (relativistic) quantum mechanical origin of the anomalous effects.

5.2. Spin–orbit coupling

The spin–orbit interaction describes the effect of an electron's orbital motion on the orientation of its spin. As for the spin itself, relativistic arguments must be used in order to understand this interaction. However, a simple classical vision of the problem gives a good grasp of the basic relevant concepts.

In an isolated atom, electrons belong to specific orbitals described by their energy and their orbital moment L. In the rest frame of the electron, the positively charged nucleus Ze moves on a stationary orbit at a certain distance creating a magnetic induction of the order of 1.5 T. The electron spin sees this field, which is proportional to L, and the corresponding Zeeman splitting defines the scale of the associated energy: $H_{\mathrm{SO}} = \lambda\mathbf{L}\cdot\mathbf{S}$. In a central potential approximation for an electron of mass m at distance r from the nucleus, the factor λ is of the form

$$\lambda = \frac{1}{2m^2rc^2}\frac{\mathrm{d}V}{\mathrm{d}r}. \quad (6)$$

The related magnitude of ΔE_{SO} is of the order of meV/atom, increasing with the atomic weight (through the potential V increasing with Z). This spin–orbit interaction is central to the way atoms are built. This can be seen through Hund's rules which maximize the total spin S and angular momentum L and, because of their mutual interaction, state that when the shell is less than half filled $J = L - S$ while when it is more than half filled $J = L + S$.

The maximum orbital moment predicted by Hund's rules for isolated atoms is greatly reduced in metals with itinerant electrons. Indeed, the orbital (and total spin) properties of atoms largely depend on the valence electrons, since every filled shell has zero total orbital (and spin) moment. Hence, electron delocalization and band formation can dramatically change the magnetic properties. Indeed, very few elements are magnetic in their bulk form compared to single atoms. For the orbital moment, delocalized electrons result in an almost complete quenching of L. Thus, there is a large difference between anisotropic properties of single atoms and of bulk compounds. However, most anisotropic magnetic properties of materials are still due to spin–orbit coupling, including magneto-crystalline anisotropy, magnetostriction and AMR.

A thorough theoretical treatment of the AMR is beyond the scope of the present paper, and can be found in the literature. We summarize here the essential ingredients, following three major works in this field: that of Mott from the 1930s for the two-channel model of conduction in transition metals [98, 99], the AMR theory proposed by Smit in the 1950s [93], and finally the 1970 calculation by Potter that updated Smit's results [94].

In transition metals, s bands result in almost free-like electrons while d bands are rather narrow. Hence, Mott pointed out that for the transition metals most of the conduction is done by s electrons. Since at the Fermi level d bands offer a very large density of states, the conducting s electrons are mainly scattered into these d bands [100]. Because the unoccupied d states are responsible for the magnetic nature of some of the transition elements, their conductivity is linked to their magnetic properties. In particular, because the d bands are spin split, the scattering lifetimes of up and down spin electrons are different. When considering that most of the scattering events preserve the electron spin, it becomes possible to describe transport in two parallel independent channels of spin up and down whose conductance can be added. This picture is widely used and has been very successful in describing the electronic transport properties of magnetic metals and alloys. However, it does not account for any anisotropy in resistance in this simple form. In 1951, Smit extended Mott's theory by introducing the spin–orbit interaction, known to lift the degeneracy of atomic orbitals [93]. This was extended to the different d bands in a solid, which have a much reduced, but nevertheless non-zero, orbital moment. Smit considered that the orbital motion of the d electrons is coupled to their spin and the crystal lattice. Because the spin–orbit interaction is in $\mathbf{S}\cdot\mathbf{L}$, spin up and spin down bands do not see the same energy shift. New d electron wavefunctions must then be recalculated and are no longer eigenfunctions of S_z since H_{SO} mixes states of opposite spins. Hence, this allows some minority spin states to be scattered into majority d bands. This mixing of states is anisotropic and results in resistivity anisotropy. Potter further refined this picture by taking a more realistic band picture for ferromagnets [94]. He was able to get an analytical expression for the spin-dependent relaxation rates and concluded that sd scattering of minority spins (i.e. the ones

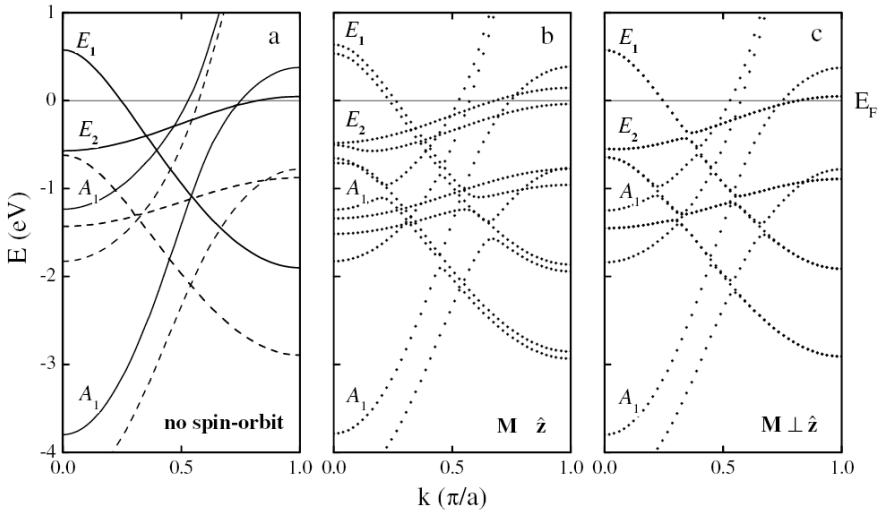

Figure 10. Calculated electronic structure of monatomic Ni wire with equilibrium interatomic distance (a) in the absence of spin–orbit interaction, (b) in the presence of spin–orbit interaction for magnetization lying along the wire axis and (c) perpendicular to the wire axis. The solid and dashed lines in (a) show the minority-spin and majority-spin bands, respectively. Reprinted with permission from [103]. Copyright 2005 from the American Physical Society.

opposite to the magnetization) is responsible for the measured AMR (with $\rho_{\parallel} > \rho_{\perp}$). Potter was also able to show that the sign of the AMR depends directly on the band structure of the ferromagnetic material. His calculation was carried out for NiCu alloys where the Fermi energy lies near the top of the uniformly split d bands. However, a significant splitting between uppermost d bands of the same spin reinforces $\rho_{\parallel} > \rho_{\perp}$ while a low exchange energy tends to inverse the sign of the AMR. Hence, since alloying allows fine tuning of the position of the Fermi level, some alloys possess negative AMR.

Further refinements have been added, especially regarding the type of scattering considered. The models presented above were established for alloys where the scattering is by impurities, but it is expected that phonon or magnon scattering can also be anisotropic. The key summary of the physics presented is that most anisotropic properties of ferromagnets result directly form spin–orbit coupling.

5.3. Anisotropic magnetoresistance in the ballistic regime (BAMR)

The picture of AMR of bulk materials should be completely revisited if the ballistic contribution to the sample resistance becomes dominant.

Firstly, the intrinsic structural, electronic and magnetic properties of such small samples are expected to differ significantly from the bulk. For example, the quenching of the orbital contribution to magnetism found for bulk magnetic materials does not apply fully when reducing the dimensionality. Calculations for transition-metal clusters of different sizes [101] show how the orbital moment gradually goes from bulk to atomic values. Recently, Gambardella *et al* [102] measured a value of $\mu_L = 0.68\ \mu_B$ per atom for the orbital moment for monatomic Co wires, which is five times larger than the bulk value $\mu_L = 0.14\ \mu_B$. Similarly, there is an increase in the spin moment per atom from the 1.57 μ_B bulk value to 2.08 μ_B for the 1D chain. Thus dimensionality significantly affects orbital moments and spins. The magnitude of the spin–orbit coupling is also expected to increase. The factor λ, proportional to the spatial derivative of the local electric potential, should be significantly enhanced when the size of the system is reduced. One expects therefore that the spin–orbit coupling energy can be greatly enhanced in open and small geometries, especially when nearly all the involved atoms are at the surface.

Secondly, the origin of the resistance anisotropy should be revised, as the arguments of the previous paragraph rely on spin-dependent scattering properties. One should therefore extend the concepts of ballistic transport to take into account the influence of spin–orbit coupling.

A good pedagogical model can be inferred from the idealized 1D chain of atoms with perfect transmission factors and can be used to demonstrate the concept behind AMR extended to Landauer formalism. *Ab initio* calculations using pseudopotential plane wave method and symmetry arguments by Velev *et al* [103] for Ni and Co, as well as calculations by Viret *et al* [104] for Fe, have shown that the weakly dispersive bands (δ bands) arising from the coupling of nearest neighbour $3d_{xy}$ and $3d_{x^2-y^2}$ atomic orbitals are split by the spin–orbit interaction when the magnetization is parallel to the wire, and nearly degenerate when perpendicular (figure 10). The energy lifting corresponds to the energy constant λ (or 2λ) associated with the spin–orbit coupling, reaching a magnitude of 0.1 eV. Because the Fermi energy lies close to the edge of the δ bands, one of the bands gets expelled from the Fermi level when split by the spin–orbit coupling energy in the relevant geometry (M parallel to the wire). Hence, the conductance is expected to change by e^2/h in this case because for an infinite atomic wire the conductance is simply e^2/h per band crossing the Fermi level. For the specific example of figure 10 (δ bands of a Ni monatomic wire), the conductance changes from 6 e^2/h to 7 e^2/h, that is a magnitude corresponding to

experiments, and much larger than bulk AMR. This so-called ballistic anisotropic magnetoresistance (BAMR) has therefore several specific properties differentiating it from bulk AMR.

(1) BAMR relative magnitude is significantly larger than bulk AMR, with an absolute magnitude of conductance change of the order of e^2/h.
(2) BAMR angular variation should be abrupt, as conduction channels are either open or closed, in contrast with a smooth $\cos^2$ variation of bulk AMR.
(3) The sign of the BAMR can be either positive or negative. Calculations usually show that the parallel resistivity is larger than the perpendicular one (similarly to AMR), but there is no fundamental argument prohibiting the opposite, as the sign is mostly determined by the 1D subbands crossing at the Fermi level, which can increase or decrease when lifting the energy degeneracy through spin–orbit interaction.

It is clear that a 1D perfect wire is a highly idealized model. In fact, when trying to understand transport in magnetic contacts, one needs to model the atomic arrangement which constitutes the narrow neck and the corresponding electronic structure. A realistic modelling of the experiments should therefore consist of three steps: (i) the determination of possible structural arrangements when making atomic contacts, (ii) the accurate computation of the electronic and magnetic structures of the systems and (iii) the calculation of the ballistic electronic transport through the junction. So far, for magnetic contacts, these three steps have not been simultaneously carried out. However, several groups are trying to understand the magnetic and transport properties of model atomic-sized constrictions. Models based on the density functional theory allow us to calculate the electronic band structure and to infer the magnetic properties of different mesoscopic or atomic structures. In atomic contacts, this has to be carried out before one can infer the transport properties. Usually, transport is dealt with using Green functions and starting from the known local band structures.

Another key problem for comparing the simplest theory to experiments is the unknown adequacy of the hypothesis of perfectly transmitting 1D wires. Actually, the conductance calculated in infinite atomic wires made of 3D metals, of the order of 6–7 G_0, appears to be larger than the experimental ones. In atomic contacts made with the MBJ technique, conductance quantification is very unclear. Hence, any attempt to quantify transport effects in these systems has to use a conductor geometry for which quantization might be lost [38, 93]. However, the presented key arguments for occurrence of BAMR remain valid, as the δ band splitting still occurs when values of conductance near G_0 are found. There, it is found that the effect depends sensitively on the exact atomic geometry of the atoms composing the neck of the contact. In particular, the coordination of the central single atom is essential in setting the amplitude of the AMR. It is found that a low coordination enhances AMR, which is consistent with common sense thinking that would conclude that the central atom needs to be as far as possible from a bulk environment. However, a quantitative interpretation of the experimental AMR is still lacking. This is due to the extreme robustness of the s bands, which always lead to two conduction channels (one up, one down) with high transmittance for any atomic geometry. These s bands are much less sensitive to magnetism than the d bands and the resulting MR effects are significantly reduced owing to the significant s-type transmission of one minority channel. In addition, it has been argued that the orbital moment used in the calculations classically carried out in the local spin density approximation (LSDA) or Stoner-like tight-binding models greatly underestimates the orbital moment in the atomic-sized constrictions [105]. This stems from the fact that in these approaches intra-atomic electronic interactions between electrons of different orbitals are averaged, thus their orbital dependence is neglected. A full calculation without these simplifications leads to a strong enhancement of the orbital magnetic moment and of its anisotropy. This greatly affects the splitting of the minority spin δ bands at the heart of the qualitative explanation of the AMR effects [46].

5.4. Experimental findings of AMR in nanocontacts

A clear experimental indication of AMR is obtained by keeping the sample magnetically saturated and varying the angle the magnetization makes with the current. For applied magnetic fields above 1 T, the magnetic configuration of the samples is saturated, as reported by several authors. Such studies therefore eliminate the problem of positioning an atomic-size domain wall, of importance for GMR-type studies, and investigate an unambiguous magnetic configuration.

Figure 11 shows results on Fe contacts for MBJs measured at low temperatures [104, 106]. The data are very instructive as they point out the importance of the contact size: a significant effect can only be measured if the contact has a conductance not exceeding a few quanta, i.e. composed of a few atoms only. Indeed, the bottom curve corresponds to a contact of resistance value which is expected to relate to a size of approximately 10 atoms and the AMR effect is only around 1%. The top two curves correspond to an expected single atomic contact of different local arrangement and only there does one find a significantly enhanced AMR, reaching 75%. The extreme sensitivity of the amplitude of the effect is even clearer when plotting the AMR amplitude as a function of the contact resistance in a set of extensive experiments on Fe atomic contacts (figure 11). Only for conductance close to the quantum (and below it) can one observe large AMR effects. Interestingly, the AMR in the tunnelling regime can also be enhanced. With hindsight, this is not surprising because conductance in this regime is also due to overlap of atomic orbitals, albeit in their evanescent tails. Hence, large AMR effects should also be observed in close 'atomic' tunnelling. Figure 11 also reveals that the angular behaviour deviates significantly from the $\cos^2\theta$ form of the bulk materials. Instead, they tend towards a two-level shape as can be seen in the middle graph of the figure. This appears to confirm the hypothesis of sudden opening or closure of conduction channels when modifying the magnetization angle.

Even clearer two-level effects were observed on Co, with remarkably abrupt change of the conductance when sweeping

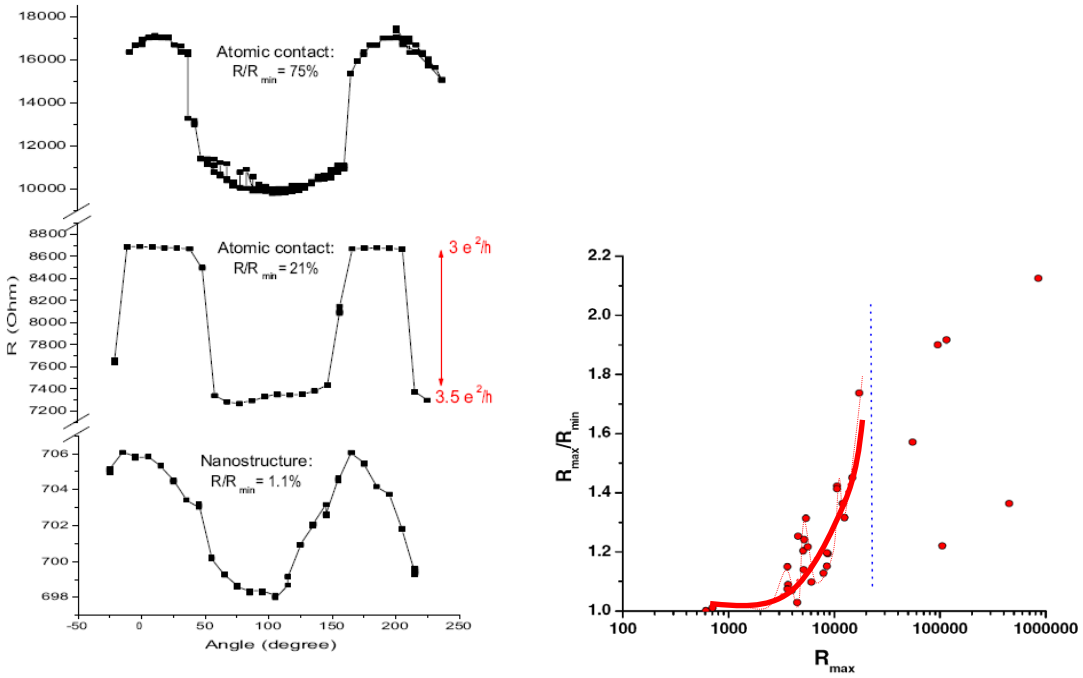

Figure 11. Dependence of the resistance on the angle between magnetization and current for different atomic Fe contacts. Right: magnitude of the amplitude of change when going from the ballistic to the tunnelling regime. Reproduced with permission from [104]. Copyright 2006 Springer.

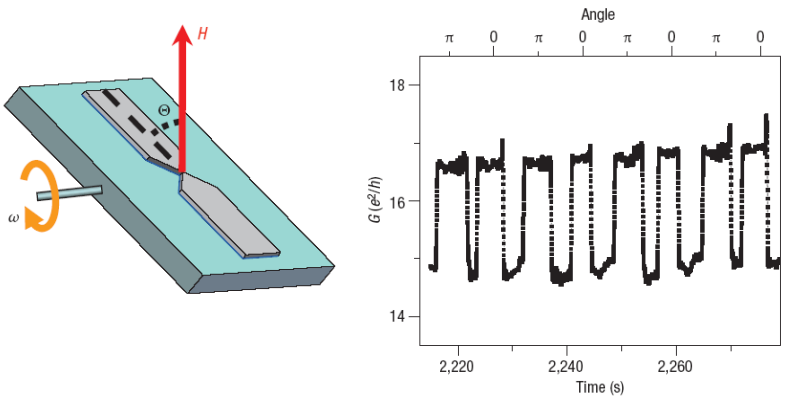

Figure 12. Anisotropic magnetoresistance of a Co nanocontact obtained by the electrochemistry technique, measured at 300 K. The sample is rotated in a magnetic field of amplitude typically 0.8–1 T. Angular curves reveal reproducible switching between two values. Reprinted by permission from Macmillan Publishers Ltd: Nature [107]. ©2007.

the angle (figure 12) [107]. Experiments performed at room temperature on ECJs revealed reproducible switching between two stable conductance values, of amplitude of order e^2/h. For this type of experiments, the sample was rotated in the magnetic field, allowing faster angular change. The sign of the effect can also be opposite. About 90% of the samples showed a typical resistance larger in the parallel configuration (figure 13(a)), but the opposite, or a more complicated effect also occurred (figures 13(b)–(d)). This set of measurements provides therefore a clear confirmation of the three predicted specific characteristics of BAMR properties described in the previous section. One should note, however, that the electrical stabilization with time and sample rotation is a challenging experiment, and closer inspection of the AMR of figure 12 indicates a non-perfect reproducibility of the angular behaviour (see the discussion in the supplement material of [107]).

The experimental findings on nanocontact AMR still reveal significant disagreement in the observed magnitude of the effect and the interpretation of the data. Bolotin *et al* studied AMR properties of EBJs at low temperatures, and reported smaller amplitude values that were strongly dependent on the applied bias voltage (figure 14) [108]. They interpreted their results with quantum fluctuations arguments, and pointed out that disorder in the nanocontact region can significantly enhance this phenomenon. The remarkable sharpness of the conductance angular transitions found on

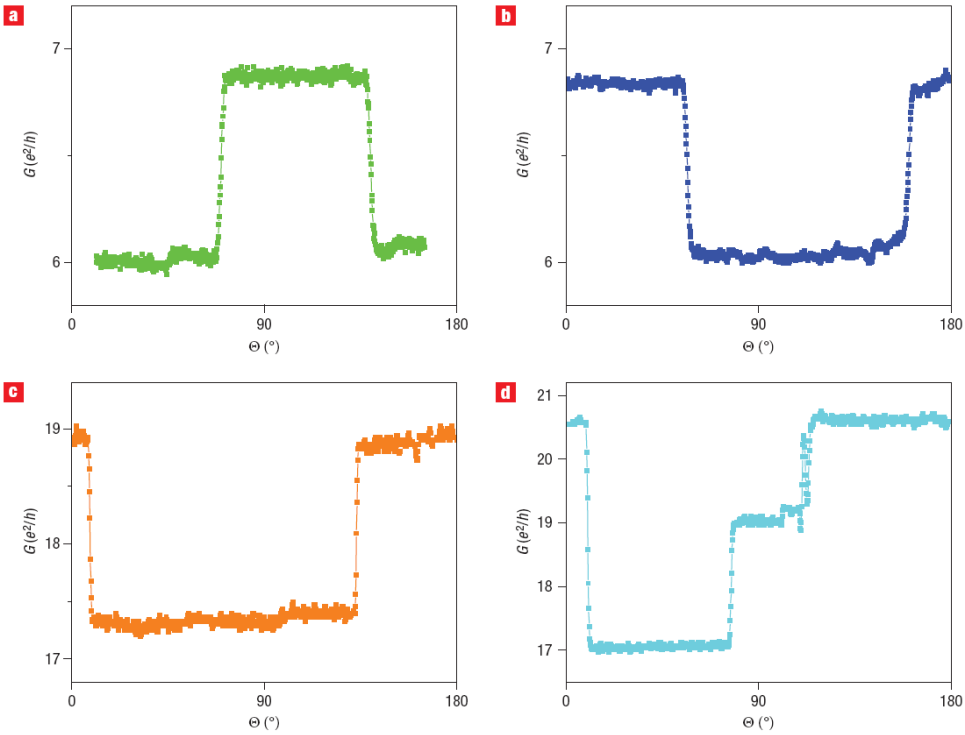

Figure 13. Anisotropic magnetoresistance of a Co nanocontact showing the diversity of curves, with a possible change of sign of the AMR ((b)–(d)), occurring for around 10% of the samples. Reprinted by permission from Macmillan Publishers Ltd: Nature [107]. ©2007.

Co samples (figure 13) is also reminiscent of fluctuations between two (or multiple) voltage levels found in electrical telegraph noise. It is known that such noise can reach large amplitudes in very small systems. It has been for example reported in point contacts [109, 110], MBJs [111], and electrochemical magnetic nanojunctions [112]. For nanocontacts, the explanation of such two-level fluctuation is based on a model of atomic rearrangements at the constriction, possibly including magnetic fluctuations when considering magnetic systems. Such an occurrence can mimic BAMR data, as recently shown by Shi and Ralph on Ni EBJs [113]. It is too early to claim that such arguments remain valid for the data of figures 11 and 12, as there was no evidence of fluctuations observed for ECJs [114]. There might be an advantage in terms of mechanical and surface stability when samples are immersed in an electrolyte [115] and fabricated by a growth process (in opposition to a breakage process). More experiments are clearly needed to clarify the issue. The observed difference between Ni and Co is also remarkable. For example, angular measurements performed on Ni ECJs did not reveal a quantum-type behaviour, but noisy features, compatible with reported occurrence of TLF [107]. Experiments on Co on MBJ and EBJ samples should help resolve the issue. Again, more systematic experiments are needed.

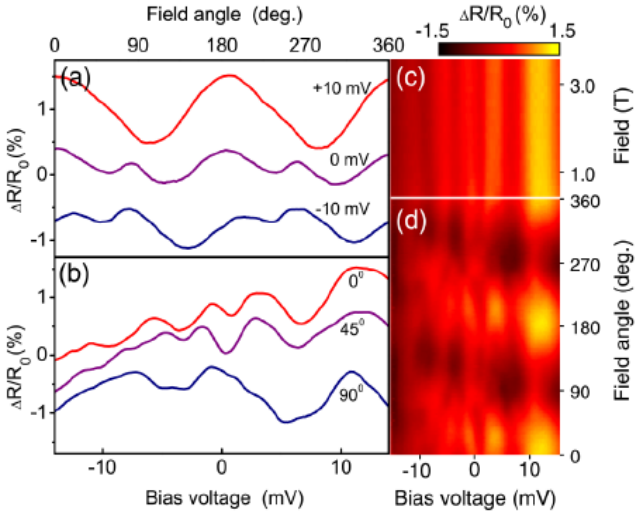

Figure 14. Variations of $R = \mathrm{d}V/\mathrm{d}I$ at 4.2 K in a sample with average zero-bias resistance of 2:6 kΩ. (a) R versus field angle at different bias voltages ($B = 0.8$ T). (b) Dependence of R on V at different fixed angles of magnetic field ($B = 0.8$ T). The curves in (a) and (b) are offset vertically. (c) R as a function of V and magnetic field strength, with field directed along the x axis. R does not have significant dependence on the magnitude of B. (d) R as a function of V and for $B = 0.8$ T. Reprinted figure with permission from [108]. Copyright (2006) from the American Physical Society.

6. Conclusions

The topic of ballistic transport in magnetic systems is still far from closed. Even though there is a general consensus for criticizing the first experiments claiming giant ballistic MR effects, a number of experimental and theoretical questions remain. At this point, it seems necessary to comment on the

term of 'ballistic magnetoresistance', which is questionable in our opinion. In a true ballistic two-terminal configuration (corresponding to figure 1), the impedance mismatch at the borders between the channel and the leads results in conductance values that are multiples of (2) e^2/h. Any deviation of the related transmission factors from unity is an indication of partial reflection, or scattering, which questions the denomination 'ballistic'. Moreover, calling an effect 'ballistic' implies, in our opinion, that it originates in the nature of transport, and not in a change of (elastic) scattering. Thus, if a band is shifted out of the Fermi level (as in the calculations for the perfect 1D model), and a conductance variation of e^2/h results, then one can invoke a ballistic effect. However, in more realistic atomic geometries, most opened channels do not have perfect transmission, i.e. the central atom of the contact represents a scattering centre. If the anisotropy of spin–orbit coupling changes the transmittance values of individual channels, i.e. the local scattering amplitude, one cannot qualify the effect of being 'ballistic' in nature. This motivated the denomination atomic anisotropic magneto-resistance (AAMR) in [104], because both cases (changes in either the number of transmission channels or the individual transmittances) originate in the atomic nature of the contact. Basically, it is argued that the magnetism due to the reduced dimension of the contact is at the origin of the AMR effect [46]. This requires atomic structures. This is however making a strong statement about the morphology of the sample, which is essentially unknown, as the only experimental insight into the structure of metallic contacts is obtained by TEM imaging, and reveals that several atoms participate in the contact [39, 55, 56]. In our opinion, there is no real satisfactory vocabulary or abbreviation, but the atomic character of the effect should be underlined.

The reviewed data reveal MR properties stable with time and reproduced when performing several sweeps of the applied magnetic field amplitude and/or direction. Our conclusions rely on several independent experiments performed on different types of samples in different environments. Our goal is to draw clear conclusions, based on converging experimental evidence.

We consider that it is now clearly established that the MR of a magnetic nanocontact does not exceed a few tens per cent when adequate precautions against mechanical artefacts and surface contaminations are taken. Furthermore, the extensive studies on MBJs provide a theoretical and experimental framework explaining such limitations. The necessity to obtain samples involving a single transmission mode of optimum transparency makes the occurrence of significant MR values highly challenging in transition metal conductors.

When magnetic contacts reach conductance values of the order of e^2/h, a systematic occurrence of anisotropy in the MR is found, of magnitude higher than the observed MR under sweeping field, and one to two orders of magnitude larger than in the bulk. Spin–orbit coupling must be invoked to explain this AMR, and independent experiments indeed reveal that spin–orbit coupling is enhanced in nanoscale systems. In the simplest theoretical picture, the spin–orbit splitting of electronic orbitals results in a change of the number of transmission modes with the angle between magnetization and current. The AMR curve in the ballistic quantum regime should therefore show an amplitude and behaviour significantly different from the bulk AMR curve. There are now a few experimental indications that this is indeed the case.

More theoretical work is still needed to achieve full quantitative understanding. Clearly, one needs to go beyond the 1D infinite chain models, which cannot reproduce non-perfect channel transmission properties. It remains unclear whether all the necessary ingredients are indeed present in the models. For instance, it is possible that the picture in which s bands provide two fully conducting channels and are only weakly magnetism dependent could be erroneous. Perhaps the large orbital magnetism or considerations linked to destructive interferences of s channels will lead to a better understanding of the MR effects.

The fundamental interplay between structural, magnetic and electronic properties significantly complicates the experiments. The occurrence of mechanical effects can still be a problem in the interpretation of the results, even when all experimental precautions are taken to minimize mechanical artefacts. Atoms at surfaces are mobile, and atomic reorganizations in atomic-sized systems can always possibly occur and can even be linked to the atoms' magnetic moments. Even for stable atomic arrangements, the sensitivity of the expected AMR properties to the details of the atomic structure limits the reproducibility of the experiments. However, it now seems clear that the dominant magnetoresistive phenomenon in atomic-sized structures is anisotropic magnetoresistance.

Acknowledgments

We thank the graduate students who dedicated their thesis efforts to working towards the conclusions presented here, namely C S Yang, C Zhang and M Gabureac. We also thank the colleagues who provided laboratory help and highly valuable scientific insight: N Ianno, M Johnson, S H Liou, A Sokolov, J Redepenning, E Tsymbal, F Ott, C Fermon, X Waintal, C Barreteau, D Spanjaard, M-C Desjonquères and G Autès.

This research was partly supported by the NSF Materials Research Science and Engineering Centers programme DMR-0213808 and by the French Agence Nationale de la Recherche 'Chaire d'excellence' programme.

References

[1] Levy P M 1994 Giant magnetoresistance in magnetic layered and granular materials *Solid State Physics* vol 47, ed H Ehrenreich and D Turnbull (Cambridge, MA: Academic) pp 367–462

[2] Barthélémy A, Fert A and Petroff F 1999 *Handbook of Ferromagnetic Materials* vol 12, ed K H J Buschow (Amsterdam: Elsevier Science) chapter 1 (Giant Magnetoresistance in Magnetic Multilayers)

[3] Tsymbal E Y and Pettifor D G 2001 Perspectives of giant magnetoresistance *Solid State Physics* vol 56, ed H Ehrenreich and F Spaepen (Cambridge, MA: Academic) pp 113–237

[4] Schep K M, Kelly P J and Bauer G E W 1995 Giant magnetoresistance without defect scattering *Phys. Rev. Lett.* **74** 586

[5] Schep K M, Kelly P J and Bauer G E W 1998 Ballistic transport and electronic structure *Phys. Rev.* B **57** 8907

[6] Jansen A G M, Gelder A P V and Wyder P 1980 Point-contact spectroscopy in metals *J. Phys. C: Solid State Phys.* **13** 6073

[7] Tsoi M V, Jansen A G M and Bass J 1997 Search for point-contact giant magnetoresistance in Co/Cu multilayers *The 41st Annual Conf. on Magnetism and Magnetic Materials (Atlanta, GA)* (New York: AIP) p 8

[8] Wellock K, Theeuwen S J C H, Caro J, Gribov N N, Van Gorkom R P, Radelaar S, Tichelaar F D, Hickey B J and Marrows C H 1999 Giant magnetoresistance of magnetic multilayer point contacts *Phys. Rev.* B **60** 10291

[9] García N, Muñoz M and Zhao Y W 1999 Magnetoresistance in excess of 200% in ballistic Ni nanocontacts at room temperature and 100 Oe *Phys. Rev. Lett.* **82** 2923

[10] García N, Rohrer H, Saveliev I G and Zhao Y W 2000 Negative and positive magnetoresistance manipulation in an electrodeposited nanometer Ni contact *Phys. Rev. Lett.* **85** 3053

[11] García N, Muñoz M, Qian G G, Rohrer H, Saveliev I G and Zhao Y W 2001 Ballistic magnetoresistance in a magnetic nanometer sized contact: an effective gate for spintronics *Appl. Phys. Lett.* **79** 4550–2

[12] García N, Qiang G G and Saveliev I G 2002 Balistic magnetoresistance in nanocontacts electrochemically grown between macro- and microscopic ferromagnetic electrodes *Appl. Phys. Lett.* **80** 1785–7

[13] Versluijs J J, Bari M A and Coey J M D 2001 Magnetoresistance of half-metallic oxide nanocontacts *Phys. Rev. Lett.* **87** 026601

[14] Chung S H, Muñoz M, García N, Egelhoff W F and Gomez R D 2002 Universal scaling of ballistic magnetoresistance in magnetic nanocontacts *Phys. Rev. Lett.* **89** 287203

[15] Bruno P 1999 Geometrically constrained magnetic wall *Phys. Rev. Lett.* **83** 2425

[16] Tatara G, Zhao Y W, Muñoz M and García N 1999 Domain wall scattering explains 300% ballistic magnetoconductance of nanocontacts *Phys. Rev. Lett.* **83** 2030

[17] Van Hoof J B A N, Schep K M, Brataas A, Bauer G E W and Kelly P J 1999 Ballistic electron transport through magnetic domain walls *Phys. Rev.* B **59** 138

[18] Brataas A, Tatara G and Bauer G E W 1999 Ballistic and diffuse transport through a ferromagnetic domain wall *Phys. Rev.* B **60** 3406

[19] Imamura H, Kobayashi N, Takahashi S and Maekawa S 2000 Conductance quantization and magnetoresistance in magnetic point contacts *Phys. Rev. Lett.* **84** 1003

[20] Velev J and Butler W H 2004 Domain-wall resistance in metal nanocontacts *Phys. Rev.* B **69** 094425

[21] Zhuravlev M Y, Tsymbal E Y, Jaswal S S, Vedyayev A V and Dieny B 2003 Spin blockade in ferromagnetic nanocontacts *Appl. Phys. Lett.* **83** 3534–6

[22] Yang Z, Qi Y and Zhang S 2004 Magnetoresistance and resistance of magnetic nanoconstriction *Phys. Rev.* B **70** 094404

[23] Chopra H D and Hua S Z 2002 Ballistic magnetoresistance over 3000% in Ni nanocontacts at room temperature *Phys. Rev.* B **66** 020403

[24] Hua S Z and Chopra H D 2003 100 000% ballistic magnetoresistance in stable Ni nanocontacts at room temperature *Phys. Rev.* B **67** 060401

[25] Chopra H D, Sullivan M R, Armstrong J N and Hua S Z 2005 The quantum spin-valve in cobalt atomic point contacts *Nat. Mater.* **4** 832

[26] Brumfiel G 2003 Magnetic effect sends physicists into a spin *Nature* **426** 110

[27] Egelhoff J W F, Gan L, Ettedgui H, Kadmon Y, Powell C J, Chen P J, Shapiro A J, Mcmichael R D, Mallett J J, Moffat T P, Stiles M D and Svedberg E B 2004 Artifacts in ballistic magnetoresistance measurements (invited) *J. Appl. Phys.* **95** 7554–9

[28] Agrait N, Yeyati A L and Van Ruitenbeek J M 2003 Quantum properties of atomic-sized conductors *Phys. Rep.* **377** 81

[29] Vogel E 2007 Technology and metrology of new electronic materials and devices *Nat. Nanotechnol.* **2** 25

[30] Datta S and Das B 1990 Electronic analog of the electro-optic modulator *Appl. Phys. Lett.* **56** 665

[31] Rashba E I and Efros A L 2003 Orbital mechanisms of electron-spin manipulation by an electric field *Phys. Rev. Lett.* **91** 126405

[32] Zutic I, Fabian J and Sarma S D 2004 Spintronics: fundamentals and applications *Rev. Mod. Phys.* **76** 323

[33] Schmidt G 2005 Concepts for spin injection into semiconductors—a review *J. Phys. D: Appl. Phys.* **38** R107

[34] Sharvin Y V 1965 A possible method for studying Fermi surfaces *Sov. Phys.—JETP* **21** 655

[35] Landauer R 1957 Spatial variation of currents and fields due to localized scatterers in metallic conduction *IBM J. Res. Dev.* **1** 223

[36] Van Wees B J, Van Houten H, Beenakker C W J, Williamson J G, Kouwenhoven L P, Van der Marel D and Foxon C T 1988 Quantized conductance of point contacts in a two-dimensional electron gas *Phys. Rev. Lett.* **60** 848

[37] Wharam D A, Thornton T J, Newbury R, Pepper M, Ahmed H, Frost J E F, Hasko D G, Peacock D C, Ritchie D A and Jones G A C 1988 One-dimensional transport and the quantisation of the ballistic resistance *J. Phys. C: Solid State Phys.* **21** L209

[38] Krans J M, van Ruitenbeek J M, Fisun V V, Yanson I K and De Jongh L J 1995 The signature of conductance quantization in metallic point contacts *Nature* **375** 767

[39] Ohnishi H, Kondo Y and Takayanagi K 1998 Quantized conductance through individual rows of suspended gold atoms *Nature* **395** 780

[40] Scheer E, Agraït N, Cuevas J C, Yeyati A L, Ludoph B, Martín-Rodero A, Bollinger G R, van Ruitenbeek J M and Urbina C 1998 The signature of chemical valence in the electrical conduction through a single-atom contact *Nature* **394** 154

[41] Scheer E, Joyez P, Esteve D, Urbina C and Devoret M H 1997 Conduction channel transmissions of atomic-size aluminum contacts *Phys. Rev. Lett.* **78** 3535

[42] Zhuravlev M Y, Tsymbal E Y, Jaswal S S, Vedyayev A V and Dieny B 2003 Spin blockade in ferromagnetic nanocontacts *Appl. Phys. Lett.* **83** 3534–6

[43] Nakanishi K and Nakamura Y O 2000 Effect of a domain wall on conductance quantization in a ferromagnetic nanowire *Phys. Rev.* B **61** 11278

[44] Autes G, Barreteau C, Spanjaard D and Desjonquieres M-C 2006 Magnetism of iron: from the bulk to the monatomic wire *J. Phys.: Condens. Matter* **18** 6785

[45] Burton J D, Kashyap A, Zhuravlev M Y, Skomski R, Tsymbal E Y, Jaswal S S, Mryasov O N and Chantrell R W 2004 Field-controlled domain-wall resistance in magnetic nanojunctions *Appl. Phys. Lett.* **85** 251

[46] Autes G, Barreteau C, Desjonqueres M C, Spanjaard D and Viret M 2007 Giant orbital moments are responsible for the anisotropic magnetoresistance of atomiccontacts

[47] Jacob D 2007 *PhD Thesis* University of Alicante

[48] Gabureac M, Viret M, Ott F and Fermon C 2004 Magnetoresistance in nanocontacts induced by magnetostrictive effects *Phys. Rev.* B **69** 100401

[49] Yang C S 2004 *PhD Thesis* University of Nebraska Lincoln

[50] van Ruitenbeek J M, Alvarez A, Pineyro I, Grahmann C, Joyez P, Devoret M H, Esteve D and Urbina C 1996 Adjustable nanofabricated atomic size contacts *Rev. Sci. Instrum.* **67** 108

[51] Costa-Kramer J L 1997 Conductance quantization at room temperature in magnetic and nonmagnetic metallic nanowires *Phys. Rev.* B **55** R4875

[52] Untiedt C, Dekker D M T, Djukic D and van Ruitenbeek J M 2004 Absence of magnetically induced fractional quantization in atomic contacts *Phys. Rev.* B **69** 081401

[53] Ohnishi H, Kondo Y and Takayanagi K 1998 Quantized conductance through individual rows of suspended gold atoms *Nature* **395** 780

[54] Ono T, Ooka Y, Miyajima H and Otani Y 1999 $2e^2/h$ to e^2/h switching of quantum conductance associated with a change in nanoscale ferromagnetic domain structure *Appl. Phys. Lett.* **75** 1622–4

[55] Rodrigues V, Fuhrer T and Ugarte D 2000 Signature of atomic structure in the quantum conductance of gold nanowires *Phys. Rev. Lett.* **85** 4124

[56] Rodrigues V, Bettini J, Silva P C and Ugarte D 2003 Evidence for spontaneous spin-polarized transport in magnetic nanowires *Phys. Rev. Lett.* **91** 096801

[57] Park H, Lim A K L, Alivisatos A P, Park J and Mceuen P L 1999 Fabrication of metallic electrodes with nanometer separation by electromigration *Appl. Phys. Lett.* **75** 301

[58] Park J, Pasupathy A N, Goldsmith J I, Chang C, Yaish Y, Petta J R, Rinkoski M, Sethna J P, Abruna H D, Mceuen P L and Ralph D C 2002 Coulomb blockade and the Kondo effect in single-atom transistors *Nature* **417** 722

[59] Liang W, Shores M P, Bockrath M, Long J R and Park H 2002 Kondo resonance in a single-molecule transistor *Nature* **417** 725

[60] Pasupathy A N, Bialczak R C, Martinek J, Grose J E, Donev L A K, Mceuen P L and Ralph D C 2004 The Kondo effect in the presence of ferromagnetism *Science* **306** 86

[61] Bowman M, Anaya A, Korotkov A L and Davidovic D 2004 Localization and capacitance fluctuations in disordered Au nanojunctions *Phys. Rev.* B **69** 205405

[62] Anaya A, Bowman M, Korotkov A L and Davidovic D 2005 Spin-based quantum interference effects and dephasing in strongly disordered Au nanobridges *Phys. Rev.* B **72** 035452

[63] Sordan R, Balasubramanian K, Burghard M and Kern K 2005 Coulomb blockade phenomena in electromigration break junctions *Appl. Phys. Lett.* **87** 013106

[64] Houck A A, Labaziewicz J, Chan E K, Folk J A and Chuang I L 2005 Kondo effect in electromigrated gold break junctions *Nano Lett.* **5** 1685–8

[65] Heersche H B, De Groot Z, Folk J A, Kouwenhoven L P, Van der Zant H S J, Houck A A, Labaziewicz J and Chuang I L 2006 Kondo effect in the presence of magnetic impurities *Phys. Rev. Lett.* **96** 017205

[66] Esen G and Fuhrer M S 2005 Temperature control of electromigration to form gold nanogap junctions *Appl. Phys. Lett.* **87** 263101

[67] Trouwborst M L, Van der Molen S J and Van Wees B J 2006 The role of Joule heating in the formation of nanogaps by electromigration *J. Appl. Phys.* **99** 114316

[68] Taychatanapat T, Bolotin K I, Kuemmeth F and Ralph D C 2007 Imaging electromigration during the formation of break junctions *Nano Lett.* **7** 652–6

[69] Wu Z M, Steinacher M, Huber R, Calame M, Van der Molen S J and Schonenberger C 2007 Feedback controlled electromigration in four-terminal nanojunctions *Appl. Phys. Lett.* **91** 053118

[70] Bolotin K I, Kuemmeth F, Pasupathy A N and Ralph D C 2006 From ballistic transport to tunneling in electromigrated ferromagnetic breakjunctions *Nano Lett.* **6** 123–7

[71] Keane Z K, Yu L H and Natelson D 2006 Magnetoresistance of atomic-scale electromigrated nickel nanocontacts *Appl. Phys. Lett.* **88** 062514

[72] Strachan D R, Smith D E, Johnston D E, Park T H, Therien M J, Bonnell D A and Johnson A T 2005 Controlled fabrication of nanogaps in ambient environment for molecular electronics *Appl. Phys. Lett.* **86** 043109

[73] Morpurgo A F, Marcus C M and Robinson D B 1999 Controlled fabrication of metallic electrodes with atomic separation *Appl. Phys. Lett.* **74** 2084

[74] Kervennic Y V, Van der Zant H S J, Morpurgo A F, Gurevich L and Kouwenhoven L P 2002 Nanometer-spaced electrodes with calibrated separation *Appl. Phys. Lett.* **80** 321

[75] Chen F, Qing Q, Ren L, Wu Z and Liu Z 2005 Electrochemical approach for fabricating nanogap electrodes with well controllable separation *Appl. Phys. Lett.* **86** 123105

[76] Qing Q, Chen F, Li P, Tang W, Wu Z and Liu Z 2005 Finely tuning metallic nanogap size with electrodeposition by utilizing high-frequency impedance in feedback *Angew. Chem.* **117** 7949–53

[77] Xiang J, Liu B, Wu S-T, Ren B, Yang F-Z, Mao B-W, Chow Y L and Tian Z-Q 2005 A controllable electrochemical fabrication of metallic electrodes with a nanometer/angstrom-sized gap using an electric double layer as feedback *Angew. Chem. Int. Edn* **44** 1265–8

[78] Mészáros G, Kronholz S, Karthäuser S, Mayer D and Wandlowski T 2007 Electrochemical fabrication and characterization of nanocontacts and nm-sized gaps *Appl. Phys.* A **87** 569

[79] Yang C S, Thiltges J, Doudin B and Johnson M 2002 *In situ* monitoring of quantum conductance in electrodeposited magnetic point contacts *J. Phys.: Condens. Matter* **14** L765–71

[80] Elhoussine F, Matefi-Tempfli S, Encinas A and Piraux L 2002 Conductance quantization in magnetic nanowires electrodeposited in nanopores *Appl. Phys. Lett.* **81** 1681–3

[81] Shu C, Li C Z, He H X, Bogozi A, Bunch J S and Tao N J 2000 Fractional conductance quantization in metallic nanoconstrictions under electrochemical potential control *Phys. Rev. Lett.* **84** 5196

[82] Deshmukh M M, Prieto A L, Gu Q and Park H 2003 Fabrication of asymmetric electrode pairs with nanometer separation made of two distinct metals *Nano Lett.* **3** 1383–5

[83] Paunovic M and Schlesinger M 2006 *Fundamentals of Electrochemical Deposition* (Hoboken: Wiley)

[84] Boussaad S and Tao N J 2002 Atom-size gaps and contacts between electrodes fabricated with a self-terminated electrochemical method *Appl. Phys. Lett.* **80** 2398

[85] Ozatay O, Chalsani P, Emley N C, Krivorotov I N and Buhrman R A 2004 Magnetoresistance and magnetostriction effects in ballistic ferromagnetic nanoconstrictions *J. Appl. Phys.* **95** 7315–7

[86] Montero M I, Dumas R K, Liu G, Viret M, Stoll O M, Macedo W A A and Schuller I K 2004 Magnetoresistance of mechanically stable Co nanoconstrictions *Phys. Rev.* B **70** 184418

[87] Viret M, Berger S, Gabureac M, Ott F, Olligs D, Petej I, Gregg J F, Fermon C, Francinet G and Goff G L 2002 Magnetoresistance through a single nickel atom *Phys. Rev.* B **66** 220401

[88] Yang C S, Zhang C, Redepenning J and Doudin B 2004 *In situ* magnetoresistance of Ni nanocontact *Appl. Phys. Lett.* **84** 2865

[89] Mallett J J, Svedberg E B, Ettedgui H, Moffat T P and Egelhoff J W F 2004 Absence of ballistic

magnetoresistance in Ni contacts controlled by an electrochemical feedback system *Phys. Rev.* B **70** 172406
[90] Yang C S, Zhang C, Redepenning J and Doudin B 2005 Anisotropy magnetoresistance of quantum ballistic nickel nanocontacts *J. Magn. Magn. Mater.* **286** 186
[91] Wei H X, Wang T X, Clifford E, Langford R M, Han X F and Coey J M D 2006 Magnetoresistance of nickel nanocontacts fabricated by different methods *J. Appl. Phys.* **99** 08C512
[92] Thomson W 1856 On the electro-dynamic qualities of metals: effects of magnetization on the electric conductivity of nickel and of iron *Proc. R. Soc.* **8** 546
[93] Smit J 1951 Magnetoresistance of ferromagnetic metals and alloys at low temperatures *Physica* **17** 612
[94] Potter R I 1974 Magnetoresistance anisotropy in ferromagnetic NiCu alloys *Phys. Rev.* B **10** 4626
[95] Campbell I A and Fert A 1982 Transport proprieties of ferromagnets *Ferromagnetic Materials* (Amsterdam: North-Holland)
[96] Mcguire T and Potter R 1975 Anisotropic magnetoresistance in ferromagnetic 3d alloys *IEEE Trans. Magn.* **11** 1018
[97] Fert A and Campbell I A 1976 Electrical resistivity of ferromagnetic nickel and iron based alloys *J. Phys. F: Met. Phys.* **6** 849
[98] Mott N F 1936 The electrical conductivity of transition metals *Proc. R. Soc.* A **153** 699
[99] Mott N F 1936 The resistance and thermoelectric properties of the transition metals *Proc. R. Soc.* A **156** 368
[100] Mott N F 1964 Electrons in transition metals *Adv. Phys.* **13** 325
[101] Guirado-López R A, Dorantes-Dávila J and Pastor G M 2003 Orbital magnetism in transition-metal clusters: from Hund's rules to bulk quenching *Phys. Rev. Lett.* **90** 226402
[102] Gambardella P, Dallmeyer A, Maiti K, Malagoli M C, Eberhardt W, Kern K and Carbone C 2002 Ferromagnetism in one-dimensional monatomic metal chains *Nature* **416** 301
[103] Velev J, Sabirianov R F, Jaswal S S and Tsymbal E Y 2005 Ballistic anisotropic magnetoresistance *Phys. Rev. Lett.* **94** 127203
[104] Viret M, Gabureac M, Ott F, Fermon C, Barreteau C, Autes G and Guirado-Lopez R 2006 Giant anisotropic magneto-resistance in ferromagnetic atomic contacts *Eur. Phys. J.* B **51** 1
[105] Desjonqueres M C, Barreteau C, Autes G and Spanjaard D 2007 Orbital contribution to the magnetic properties of nanowires: is the orbital polarization ansatz justified? *Eur. Phys. J.* B **55** 23–7
[106] Gabureac M 2004 *PhD Thesis* Université P et M Curie, Paris VI
[107] Sokolov A, Zhang C, Tsymbal E Y, Redepenning J and Doudin B 2007 Quantized magnetoresistance in atomic-size contacts *Nat. Nanotechnol.* **2** 171
[108] Bolotin K I, Kuemmeth F and Ralph D C 2006 Anisotropic magnetoresistance and anisotropic tunneling magnetoresistance due to quantum interference in ferromagnetic metal break junctions *Phys. Rev. Lett.* **97** 127202
[109] Ralls K S, Ralph D C and Buhrman R A 1989 Individual-defect electromigration in metal nanobridges *Phys. Rev.* B **40** 11561
[110] Weissman M B 1988 1/f noise and other slow, nonexponential kinetics in condensed matter *Rev. Mod. Phys.* **60** 537
[111] Brom H E V D, Yanson A I and Ruitenbeek J M V 1998 Characterization of individual conductance steps in metallic quantum point contacts *Physica* B **252** 69
[112] Doudin B, Redmond G, Gilbert S E and Ansermet J P 1997 Magnetoresistance governed by fluctuations in ultrasmall Ni/NiO/Co junctions *Phys. Rev. Lett.* **79** 933
[113] Shi S F and Ralph D C 2007 Atomic motion in ferromagnetic break junctions *Nat. Nanotechnol.* **2** 522
[114] Sokolov A, Zhang C, Tsymbal E Y, Redepenning J and Doudin B 2007 *Nat. Nanotechnol.* **9** 522
[115] Zheng T, Jia H, Wallace R M and Gnade B E 2006 Stabilization of Au quantum point contacts by self-assembled monolayers *Appl. Surf. Sci.* **252** 8261